

Simulating (electro)hydrodynamic effects in colloidal dispersions: smoothed profile method

Yasuya Nakayama^{1,a}, Kang Kim², and Ryoichi Yamamoto^{3,4}

¹ Department of Chemical Engineering, Kyushu University, Fukuoka 819-0395, Japan

² Department of Computational Molecular Science, Institute for Molecular Science, Myodaiji, Okazaki, Aichi 444-8585, Japan

³ Department of Chemical Engineering, Kyoto University, Kyoto 615-8510, Japan

⁴ CREST, Japan Science and Technology Agency - 4-1-8 Honcho Kawaguchi, Saitama 332-0012, Japan

Received: date / Revised version: date

Abstract. We have proposed a direct simulation scheme for colloidal dispersions in a Newtonian solvent [Phys.Rev.E **71**,036707 (2005)]. An improved formulation called "Smoothed Profile (SP) method" is presented in which a simultaneous time-marching for host fluid and colloids is accomplished. SP method as a direct numerical simulation of particulate flows provides a coupling scheme between continuum fluid dynamics and rigid-body dynamics through smoothed profile of colloidal particles. Moreover, the improved formulation includes an extension to incorporate multi-component fluids, such systems as charged colloids in electrolyte solutions. Dynamics of colloidal dispersions is solved as much computational cost as required for solving non-particulate flows. Numerical results which assess hydrodynamic interactions of colloidal dispersions are presented to validate SP method. SP method is not restricted to particular constitutive models of the host fluids. Henceforth, it can be applicable to colloidal dispersions in complex fluids.

PACS. 47.11.-j Computational methods in fluid dynamics – 82.70.-y Disperse systems; complex fluids – 82.20.Wt Computational modeling; simulation

1 Introduction

Interparticle interactions in colloidal dispersions mainly consist of thermodynamic potential interactions and hy-

drodynamic interactions [1,2,3]. Whereas the former works in both static and dynamic situations, the latter works solely in dynamic situation. Although the thermodynamic interactions have been studied extensively and summa-

^a e-mail: ynakayama@chem-eng.kyushu-u.ac.jp

ritized as a concept of the effective interaction [4], the nature of dynamic interactions are poorly understood. Since the hydrodynamic interaction is essentially long-ranged, many-body effect, it is extremely difficult to study its role by means of analytical way alone. Numerical simulations can aid to investigate fundamental role of hydrodynamic interaction in colloidal dynamics.

In these decades, various simulations for particulate flow have been developed in most simple situation where a host fluid is Newtonian [5, 6, 7, 8, 9, 10, 11, 12, 13]. However, all those schemes are not necessarily suitable for problems with non-Newtonian host fluids or solvents with internal microstructures, which are practically more important cases. Hydrodynamic simulations of ions and/or charged colloids have been proposed by making use of above schemes [14, 15, 16, 17, 18, 19]. Nonetheless, tractability and physical validity of their modeling are still controversial.

In this article, we propose a direct simulation scheme for colloidal dispersions which is applicable to most constitutive models of the host fluids. We call it "Smoothed Profile (SP) method" since the original sharp interface between colloids and a solvent are replaced with an effective smoothed interface with finite thickness [7, 20]. We formulate a computational method to couple particle dynamics and hydrodynamics of the solvent. A fixed grid is used in both the solvent and the particle domains. Introduction of a smoothed profile makes it possible to realize stable and efficient implementation of our scheme. The numerical implementation for Newtonian solvents and electrolyte

solutions as a specific example of multi-component fluids is outlined. Various test cases which verifies the SP method and assess hydrodynamic interactions are presented.

2 Dynamics of a multi-component solvent and colloids

2.1 Hydrodynamics of multi-component fluids

We first give a brief description of multi-component fluid equations keeping our mind on a specific application to electrolyte solutions. Consider N (possibly ionic) solute species, every concentration, C_α of α th species, satisfies the conservation law:

$$\partial_t C_\alpha + \nabla \cdot C_\alpha \mathbf{v}_\alpha + \nabla \cdot \mathbf{g}_\alpha = 0, \quad (1)$$

where \mathbf{v}_α is the velocity of α th solute and \mathbf{g}_α is a random current. Since the inertial time scales of the solute molecules are extremely small, the velocity of α th solute is decomposed to the velocity of solvent \mathbf{v} and diffusive current arising from the chemical potential gradient $\nabla \mu_\alpha$ as

$$\mathbf{v}_\alpha = \mathbf{v} - \Gamma_\alpha \nabla \mu_\alpha, \quad (2)$$

where $\Gamma_\alpha k_B T$ is diffusivity of α th ion, k_B the Boltzmann constant and T the temperature. The random current should satisfy the following fluctuation-dissipation relation, $\langle g_{\alpha,i}(\mathbf{x}, t) g_{\beta,j}(\mathbf{x}', t') \rangle = 2(k_B T)^2 \Gamma_\alpha \delta_{\alpha\beta} \delta_{ij} \delta(\mathbf{x} - \mathbf{x}') \delta(t - t')$ [21]. Here, for the sake of simplicity, we focused on the case where cross diffusion of different solutes is neglected. The momentum conservation implies the velocity of solvent follows the Navier-Stokes equation of incompressible

flow with the source term from solutes:

$$\nabla \cdot \mathbf{v} = 0, \quad (3)$$

$$\rho(\partial_t + \mathbf{v} \cdot \nabla) \mathbf{v} = -\nabla p + \eta \nabla^2 \mathbf{v} - \sum_{\alpha} C_{\alpha} \nabla \mu_{\alpha} + \nabla \cdot \mathbf{s}, \quad (4)$$

where ρ is the total mass density of the fluid, p the pressure, η the shear viscosity of the fluid, and \mathbf{s} a random stress satisfying the fluctuation-dissipation relation, $\langle s_{ik}(\mathbf{x}, t) s_{jl}^{\text{as}}(\mathbf{x}', t') \rangle =$

$$2k_B T \eta (\delta_{ij} \delta_{kl} + \delta_{il} \delta_{kj}) \delta(\mathbf{x} - \mathbf{x}') \delta(t - t') [21].$$

Above set of equations is closed when a set of chemical potentials $\{\mu_{\alpha}\}$ are given and describes the dynamics of a multi-component fluid. For a specific application to electrolyte, we consider the Poisson–Nernst–Planck equation for a chemical potential:

$$\mu_{\alpha}(\{C_1, \dots, C_N\}) = k_B T \log C_{\alpha} + Z_{\alpha} e (\Phi - \mathbf{E}^{\text{ext}} \cdot \mathbf{x}), \quad (5)$$

$$\epsilon \nabla^2 \Phi = -\rho_e, \quad (6)$$

which describes the Poisson–Boltzmann distribution for ions in its equilibrium state, where Z_{α} is the valence of α th ion, e is the elementary charge, Φ is the electrostatic potential, \mathbf{E}^{ext} is the external field, ϵ is the dielectric constant of the fluid, and ρ_e is the charge density field. This set of equations corresponds to the electrokinetic equations appeared in standard textbooks [3].

2.2 Colloids in electrolyte solutions

Dynamics of colloids is maintained by the force exerted by the solvent. Consider monodisperse spherical colloids with a radius a , a mass M_p , and a moment of inertia

\mathbf{I}_p , momentum conservation between the fluid and the i th colloid implies the hydrodynamic force and torque

$$\mathbf{F}_i^H = \int (\mathbf{d}\mathbf{S}_i \cdot \boldsymbol{\sigma}), \quad \mathbf{N}_i^H = \int (\mathbf{x} - \mathbf{R}_i) \times (\mathbf{d}\mathbf{S}_i \cdot \boldsymbol{\sigma}), \quad (7)$$

on it, where \mathbf{R}_i is the center of mass, $\int \mathbf{d}\mathbf{S}_i(\dots)$ indicates the surface integral on i th colloid, $\boldsymbol{\sigma}$ is the stress tensor of the fluid. For the electrokinetic equations, the stress reads

$$\boldsymbol{\sigma} = -p \mathbf{I} + \boldsymbol{\sigma}' + \boldsymbol{\sigma}^{\text{st}} + \mathbf{s}, \quad (8)$$

in which $\boldsymbol{\sigma}' = \eta (\nabla \mathbf{v} + (\nabla \mathbf{v})^T)$ is the dissipative stress, and $\boldsymbol{\sigma}^{\text{st}} = \epsilon \{ \mathbf{E} \mathbf{E} - (|\mathbf{E}|^2 / 2) \mathbf{I} \}$ is the Maxwell stress with the electric field $\mathbf{E} = -\nabla \Phi + \mathbf{E}^{\text{ext}}$, where \mathbf{I} is the unit tensor. The evolution of colloids follows the Newton's equation:

$$\dot{\mathbf{R}}_i = \mathbf{V}_i, \quad (9)$$

$$M_p \dot{\mathbf{V}}_i = \mathbf{F}_i^H + \mathbf{F}_i^c + \mathbf{F}_i^{\text{ext}}, \quad (10)$$

$$\mathbf{I}_p \cdot \dot{\boldsymbol{\Omega}}_i = \mathbf{N}_i^H + \mathbf{N}_i^{\text{ext}}, \quad (11)$$

where $\mathbf{F}_i^{\text{ext}}$ and $\mathbf{N}_i^{\text{ext}}$ are the external force and torque, respectively, and \mathbf{F}_i^c is the force arising from core potential of particles which prevents from colloids overlapping. Hereafter, soft-core potential of the truncated Lennard–Jones potential is adopted for \mathbf{F}_i^c . Specifically for the charged-colloid system, buoyancy is included in $\mathbf{F}_i^{\text{ext}}$, and external field on colloids is accounted by \mathbf{F}_i^H .

The colloidal particles with finite volume provides the relevant boundary conditions on the hydrodynamic equations. For the solvent velocity, no-slip condition, $\mathbf{v} = \mathbf{V}_i + \boldsymbol{\Omega}_i \times \mathbf{r}_i$ with $\mathbf{r}_i = \mathbf{x} - \mathbf{R}_i$ on the i th colloid, is assigned. For the concentration field, no-penetration condition, $\mathbf{n} \cdot$

$\nabla\mu_\alpha = 0$ where \mathbf{n} represent the unit normal to the surface of colloids, is assigned. Hydrodynamics coupled with the dynamics of colloids defines the moving-boundary-condition problem above. The usual numerical techniques of partial differential equations are hopeless to deal with dynamical evolution of many colloids since sharp interface at surface of colloids moves and henceforth the mesh points at which the boundary condition is assigned varies every discrete time step. The moving boundary condition requires huge computational costs. On the contrary, SP method formulate an efficient scheme for this kind of a moving-boundary-condition problem which only requires the same level of computational cost as required for solving uniform fluid.

3 Computational algorithm

In the SP method, quantities are defined on the entire domain which consists of the fluid domain and the particle domain. To designate the particle domain, we introduce a concentration field of colloids as $\phi(\mathbf{x}, t) = \sum_{i=1}^{N_p} \phi_i(\mathbf{x}, t)$, where $\phi_i \in [0, 1]$ is i th particle profile field which is unity at the particle domain, zero at the fluid domain and have a continuous diffuse interface at the interface domain with a finite thickness ξ . With the field ϕ , the total velocity field and concentration fields of the solutes are defined as

$$\mathbf{v} = (1 - \phi)\mathbf{v}_f + \phi\mathbf{v}_p, \quad (12)$$

$$C_\alpha = (1 - \phi)C_\alpha^*, \quad (13)$$

where $(1 - \phi)\mathbf{v}_f$ represents the velocity field of the fluid and $\phi\mathbf{v}_p(\mathbf{x}, t) = \sum_{i=1}^{N_p} \phi_i(\mathbf{x}, t) [\mathbf{V}_i(t) + \boldsymbol{\Omega}_i(t) \times \mathbf{r}_i(t)]$ is

the velocity field of the colloids. The auxiliary concentration field C_α^* is introduced which can have finite value in the particle domain whereas C_α , physical concentration field, is forced to be zero through the multiplication of $(1 - \phi)$.

The advection of ϕ is solved via $\dot{\mathbf{R}}_i = \mathbf{V}_i$ and mapping $\{\mathbf{R}_1, \dots, \mathbf{R}_{N_p}\}$ to ϕ . Henceforth the volume of the fluid and/or the solid is strictly conserved and no numerical diffusion of ϕ is occurred. In the SP method, fundamental field variables to be solved are chosen as the total velocity \mathbf{v} but not \mathbf{v}_f , and C_α^* but not C_α . This choice of the variables yields great benefit on the efficient and stable time evolution. The evolution equation of \mathbf{v} is derived based on the momentum conservation between the fluid and the particles and the rigidity of the particle velocity field \mathbf{v}_p . For the solute concentration, C_α and C_α^* are different in whether they have abrupt variation at the interface of colloids or not. Since C_α have abrupt variation, to solve its advection, cares to stabilize the evolution and to circumvent the numerical diffusion must be needed. However, the auxiliary concentration C_α^* is smooth on the entire domain and therefore can be solved without special cares on the colloid-solvent interface.

3.1 Discretization in time

A time-discretized evolution equations are derived as follows. For a simplicity of the presentation, we neglect the random currents. As a initial condition at the n th discretized time step, the position, the velocity, and the angular velocity of the colloids, $\{\mathbf{R}_i^n, \mathbf{V}_i^n, \boldsymbol{\Omega}_i^n\}$ ($i = 1, \dots, N_p$),

are mapped to ϕ^n and $\phi^n \mathbf{v}_p^n$ and $\mathbf{v}^n = (1 - \phi^n) \mathbf{v}_f + \phi^n \mathbf{v}_p^n$ satisfying the incompressibility condition on the entire domain, $\nabla \cdot \mathbf{v}^n = 0$, and $C_\alpha^{*,n}$ satisfying the charge neutrality condition, $\int d\mathbf{x} (1 - \phi^n) \sum_\alpha Z_\alpha e C_\alpha^{*,n} + \int d\mathbf{x} |\nabla \phi| e \sigma_e = 0$ where $|\nabla \phi| e \sigma_e$ represents the surface charge distribution of the colloids, are set. The current for the auxiliary concentration field is defined as

$$C_\alpha^* \mathbf{v}_\alpha = C_\alpha^* \mathbf{v} + (\mathbf{I} - \mathbf{n} \mathbf{n}) \cdot C_\alpha^* (-\Gamma_\alpha \nabla \mu_\alpha), \quad (14)$$

where $\mathbf{n}(\mathbf{x}, t)$ is the unit surface-normal vector field which has its support on the interface domain with the finite thickness ξ . In this definition of the current, the no-penetration condition is directly assigned. The auxiliary concentration are advected by this current as

$$C_\alpha^{*,n+1} = C_\alpha^{*,n} - \int_{t_n}^{t_n+h} ds \nabla \cdot C_\alpha^* \mathbf{v}_\alpha, \quad (15)$$

where h is a time increment and $t_n = nh$ is the n th discretized time. The total velocity field is updated by a fractional step approach. First, the advection and the hydrodynamic viscous stress are solved,

$$\mathbf{v}^* = \mathbf{v}^n + \int_{t_n}^{t_n+h} ds \nabla \cdot \left[\frac{1}{\rho} (-p \mathbf{I} + \boldsymbol{\sigma}') - \mathbf{v} \mathbf{v} \right], \quad (16)$$

$$\mathbf{R}_i^{n+1} = \mathbf{R}_i^n + \int_{t_n}^{t_n+h} ds \mathbf{V}_i, \quad (17)$$

with the incompressibility condition, $\nabla \cdot \mathbf{v}^* = 0$. Along the advection of the total velocity, the particle position is updated by the particle velocity. The electrostatic potential for the updated particle configuration is determined by solving the following Poisson equation,

$$\nabla^2 \Phi^{n+1} = -\rho_e^{n+1} / \epsilon, \quad (18)$$

with the charge density field, $\rho_e^{n+1} = (1 - \phi^{n+1}) \sum_\alpha Z_\alpha e C_\alpha^{*,n+1} + |\nabla \phi^{n+1}| e \sigma_e$, and the momentum change by the electrostatic field is solved as

$$\mathbf{v}^{**} = \mathbf{v}^* - h \rho_e^{n+1} \nabla \Phi^{n+1}. \quad (19)$$

At this point, the momentum conservation is all solved for the total velocity field. The rest of the updating procedure is for the rigidity constraint on the particle velocity field.

The hydrodynamic force and torque on the colloids exerted by the fluid are derived by the momentum conservation between the colloids and the fluid. The time-integrated hydrodynamic force and torque over a period h are equal to the momentum change on the particle domain:

$$\left[\int_{t_n}^{t_n+h} ds \mathbf{F}_i^H(s) \right] = \int d\mathbf{x} \rho \phi_i^{n+1} (\mathbf{v}^{**} - \mathbf{v}_p^n), \quad (20)$$

$$\left[\int_{t_n}^{t_n+h} ds \mathbf{N}_i^H(s) \right] = \int d\mathbf{x} [\mathbf{r}_i^{n+1} \times \rho \phi_i^{n+1} (\mathbf{v}^{**} - \mathbf{v}_p^n)]. \quad (21)$$

With this and other forces on the colloids, the particle velocity and angular velocity are updated as

$$\mathbf{V}_i^{n+1} = \mathbf{V}_i^n + M_p^{-1} \left[\int_{t_n}^{t_n+h} ds \mathbf{F}_i^H \right] + M_p^{-1} \int_{t_n}^{t_n+h} ds (\mathbf{F}_i^c + \mathbf{F}^{ext}), \quad (22)$$

$$\boldsymbol{\Omega}_i^{n+1} = \boldsymbol{\Omega}_i^n + \mathbf{I}_p^{-1} \cdot \left[\int_{t_n}^{t_n+h} ds \mathbf{N}_i^H \right] + \mathbf{I}_p^{-1} \cdot \int_{t_n}^{t_n+h} ds \mathbf{N}_i^{ext}. \quad (23)$$

The resultant particle velocity field $\phi^{n+1} \mathbf{v}_p^{n+1}$ is directly enforced on the total velocity field:

$$\mathbf{v}^{n+1} = \mathbf{v}^{**} + \left[\int_{t_n}^{t_n+h} ds \phi \mathbf{f}_p \right], \quad (24)$$

$$\left[\int_{t_n}^{t_n+h} ds \phi \mathbf{f}_p \right] = \phi^{n+1} (\mathbf{v}_p^{n+1} - \mathbf{v}^{**}) - \frac{h}{\rho} \nabla p_p, \quad (25)$$

where $\phi \mathbf{f}_p$ represents the force density field which impose the rigidity constraint on the total velocity field. The pressure due to the rigidity of the particle is determined by the incompressibility condition, $\nabla \cdot \mathbf{v}^{n+1} = 0$, which leads the following Poisson equation for p_p , viz, $\nabla^2 p_p = \frac{\rho}{h} \nabla \cdot [\phi^{n+1} (\mathbf{v}_p^{n+1} - \mathbf{v}^{**})]$. We note again that, in l.h.s. of Eqs.(20),(21), and (25), the integrands $\mathbf{F}_i^H, \mathbf{N}_i^H$, and $\phi \mathbf{f}_p$ themselves are not explicitly calculated but their time integrals are solved. In other words, forces accounting solid-fluid interactions are treated in Stieltjes form.

3.2 Restriction on a time increment

For spatial discretization of hydrodynamic equations, any standard scheme, such as finite difference method, finite volume method, finite element method, spectral method, lattice Boltzmann discretization and so forth, can be used. SP method basically defines a coupling scheme between hydrodynamic equations for solvent and equations of discrete colloids. Since the treatment of the rigidity constraint of the particle velocity introduce no additional time scale, restriction to a time increment h is the same as that of uniform fluid cases. This is advantageous compared to the method adopted in refs [7,22] where the large viscosity or elasticity on the velocity in particle domain is used. For comparison, in Fluid Particle Dynamics (FPD) [7], the large viscosity of fluid particle η_c ($\gg \eta$) is introduced to accomplish the rigidity constraint. This means that the required time increment for FPD should be very small, i.e., η/η_c ($\ll 1$) of that for SP method.

Similar discussion on the restriction by the no-penetration condition in the advection-diffusion equation of solutes works out. One of the simplest treatment of the no-penetration in the particle domain is the penalty method adopted in refs [23,24] where a artificial large potential barrier for the solutes in the particle domain is introduced. The artificial potential should be at least larger than other chemical potentials to realize no-penetration of the solutes. This fact means that the artificial potential requires smaller h . Although this strategy is physically consistent, its drawback arises as numerical inefficiency. In contrast, the advection-diffusion in the SP method requires no additional time scale due to the inclusion of colloids since no-penetration condition for the solutes is directly assigned to the solute current in the finite interface domain. From the discussion above, we see that the SP method provides us with much higher numerical efficiency than other methods proposed for direct numerical simulations of colloidal dispersions.

4 Results and Discussions

4.1 Stokes drag on a periodic array of spheres in a Newtonian fluid

To verify SP method quantitatively, we have measured the steady state drag force on a periodic array of spheres in a Newtonian solvent. The velocity distribution around the colloid is depicted in Fig.1. In general, flow around a colloid is creep-flow with Reynolds number $Re = aV/\nu \ll 1$. Figure 2 shows the drag coefficient $Q(\varphi)$ defined as

$$F_D = -\frac{6\pi\eta aV}{Q(\varphi)}, \quad (26)$$

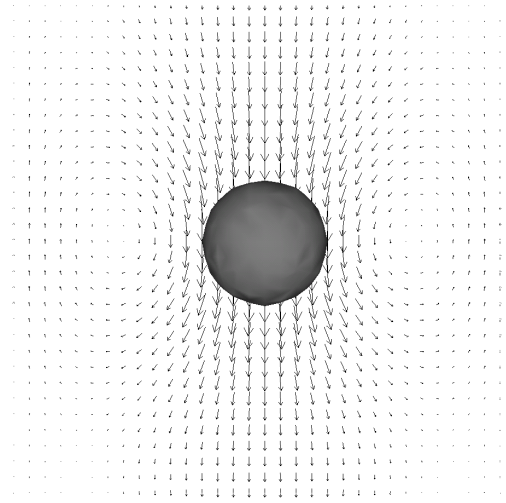


Fig. 1. Snapshot of the sedimenting colloid. The arrows indicate the velocity field.

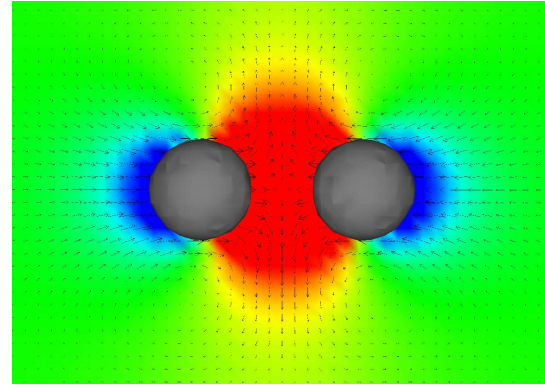


Fig. 3. Snapshot of the approaching two colloids. The arrows indicate the velocity field. The color around the colloids represents the pressure distribution: change of color from red to blue corresponds to high to low pressure.

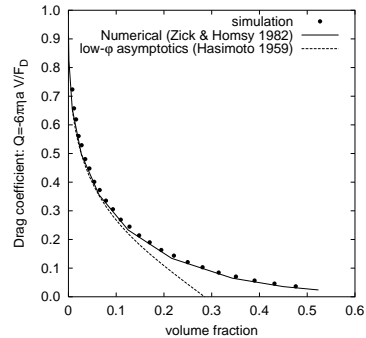


Fig. 2. Drag coefficient of a periodic array of spheres in steady Stokes flow as a function of volume fraction φ compared with the analytic result [25] (Solid line) and low- φ asymptotics [26] (dashed line). In this case, ξ is set to unity in lattice unit.

where $\varphi = (4/3)\pi(a/L)^3$ is the volume fraction in a cubic box of L^3 . Since the effect of boundary condition reaches very far in creep-flow, as higher the volume fraction, the drag become larger. Comparison of the drag coefficient with the analytic result from the Stokes equation by Zick and Homsy [25] verifies the validity of SP method over a full range of φ .

4.2 Lubrication interaction in a finite system

One of the most important effect by solvent flow is lubrication interaction between nearby particles with relative motions. The exact solution of the Stokes equation for isolated two spheres have been found [27] and provided much insight in basic physics of colloidal suspensions. However, its application to many-particle system in a way of pairwise addition needs care. For quantitative prediction of rheology of concentrated suspension, numerical results showed much difference whether shear mode of lubrication interaction is included or not [28, 29]. There exists fundamentally an ambiguity in the application of the analytic expression of isolated two spheres to many-particle system in finite domain in pairwise fashion.

We computed the squeeze lubrication interaction between two approaching spheres in a finite system. The velocity and pressure distributions are depicted in Fig.3. Figure 4(a) shows the normalized approaching velocity

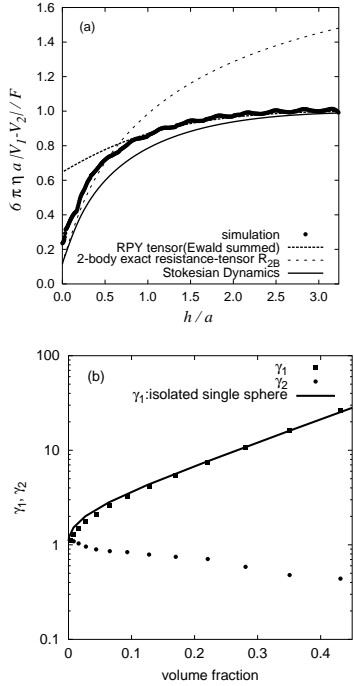


Fig. 4. (a) Relative velocity between approaching two spheres versus gap between surfaces of spheres (symbol). Slight oscillation in results by SP method came from the finite lattice spacing. In this case, ξ is set to unity in lattice unit. Curves from theories are far-field asymptotics by Rotne–Prager–Yamakawa tensor (dotted line) [30], near-field exact solution (dashed line) [27], and Stokesian Dynamics (solid line)[5]. (b) Two coefficients in squeeze interaction scaled by those of infinite dilution versus volume fraction. γ_1 (square) represents the one-body drag and γ_2 (circle) represents two-body squeeze interaction due to relative motion.

of a pair of particles versus gap h between two equal spheres compared with theories. Two asymptotics at $h \ll a$ and $h \gg a$ are from the exact solution of isolated pair [27] and Rotne–Prager–Yamakawa tensor [30], respectively. Stokesian Dynamics (SD) [5] is based on an interpolation of these two asymptotics. The simulation result nicely reproduces not only two asymptotic regimes but

also its crossover which occurs at $h/a \sim 0.7$. It is found that SD underestimates the mobility in the intermediate regime. This fact is due to the approximation adapted in SD where the ingredients are just asymptotic two-body solutions. The result indicates the relevance of our simulation demonstrating the importance of hydrodynamic interaction in a finite system.

From lubrication theory, the functional form $|V_1 - V_2|/F = (\Gamma_1(\varphi) + 2\Gamma_2(\varphi)/h)$ is assumed where $\Gamma_1(\varphi) = 6\pi\eta a\gamma_1(\varphi)$ is the one-body drag coefficient and $\Gamma_2(\varphi) = (3\pi\eta a^2/2)\gamma_2(\varphi)$ is the squeeze coefficient, and these friction coefficients can be extracted by fitting this curve. The curve from lubrication theory fits very well the results by the SP method. The reduced coefficients γ_1 and γ_2 are plotted in Fig.4(b) as a function of the volume fraction. Solid line in Fig.4(b) is from Fig.2. Although the case of a periodic array of spheres have different flow geometry from the case of two approaching spheres, the volume fraction dependence of γ_1 of these two cases are comparable. Moreover, the squeeze coefficient γ_2 is found to be a decreasing function of the volume fraction. In other words, the squeeze mode is most enhanced at infinite dilution. In the literature [2], it is pointed out that the squeeze coefficient is at least smaller than that of the exact solution for isolated pairs. These results further verified the SP method.

Although the SP method itself is an efficient scheme as a direct simulation, to construct more coarse-grained model of suspensions, such as dissipative particle dynamics, constitutive modeling, etc., the calculation by direct

simulations gives fundamental information about hydrodynamic interactions.

4.3 Sedimenting charged colloids

For a specific application to a multi-component fluid, we compute the hydrodynamic drag on sedimenting charged colloids in the absence of external electric field. In this case, sedimenting charged colloids induces a flow that determines the charge distribution different from the equilibrium case [3,31]. The skewed ion-distribution arise a polarization in electric double-layer. Moreover, double-layer deformation induces a electro-osmotic flow which makes the flow around a charged colloid different from a neutral colloid.

In this simulation, a periodic array of charged colloid in a 1:1 electrolyte solution under gravity was computed. We specify a valence of the colloids first where the counterion in the host fluid assures the charge neutrality of the whole system, and bulk concentrations of 1:1 electrolyte \bar{C}_{\pm} was determined by specifying the Debye length $\kappa^{-1} = \{4\pi\lambda_B(\bar{C}_+ + \bar{C}_-)\}^{-1/2}$. The Bjerrum length $4\pi\lambda_B = e^2/\epsilon k_B T$ was set to unity and ξ was chosen twice of a lattice unit to resolve the surface charge distribution. For simplicity, Counterion and coion was set to be of a Schmidt number 0.5. The Debye length was chosen so that the effective radius of the double-layer $a + \kappa^{-1}$ was smaller than half of the system size $L/2$. In order to make the situation clear for colloid discipline, nondimensional zeta potential $e\zeta/k_B T$ is shown in Fig.5 which should be determined by specifying κa and the valence of the col-

loid Z . Corresponding dimension of the zeta potential ζ for this simulation at 20°C is of the order of 10mV. We computed the linear response regime to the gravitational driving simply in order to observe the effect of electroosmosis on hydrodynamic drag.

We plot the sedimentation velocity scaled by that of a neutral colloid as a function of the inverse Debye length scaled by the radius of colloid in Fig. 6. As the valence of colloid or the zeta potential increase, reduction of the sedimentation velocity to that of the neutral colloid enhanced. The hydrodynamic drag of the electrolyte solution was most enhanced when the Debye length was comparable to the size of the colloids. These facts qualitatively agrees with the analytic result at infinite dilution [32,33].

The charge-density and the velocity distributions when $\kappa a = 1$ and $Z = 1000$ is depicted in Fig.7. In this case, charge distribution was not very skewed thus the counteracting electrostatic effect of double-layer polarization does not worked much. Therefore, the enhanced electrohydrodynamic drag should mainly be attributed to the friction between solvent and ions. Because of this electrohydrodynamic coupling of the momentum transfers, solvent-flow pattern around the colloid was modified from the case of neutral colloid. As a result, the viscous drag on the colloid was enhanced. This mechanism by electro-osmotic flow generally exists in colloids in electrolyte solutions.

It has been known that in the infinitely dilute system (or in thin double-layer limit) velocity decay as r^{-3} in the region of $\kappa r \gg 1$ in contrast to r^{-1} decay of the infinitely dilute neutral system where r is radial distance

from the center of the colloid [34, 35]. However, in the system size adapted in our simulation this asymptotic regime was not reached. For $\kappa r \lesssim 1$, the screened hydrodynamics regime where the velocity decays as $v \propto e^{-\kappa r}/r$ [35]. This is why the flow patterns in Figs.(1) and (6) resembles in appearance. In other words, electrohydrodynamic interaction should be in pronounced effect in small finite systems as is seen in neutral systems.

We note that charged colloid dynamics in finite volume fraction and in a range of the Debye length was effectively assessed by direct simulations like SP method. Further application of the SP method to electrophoresis of concentrated suspensions is reported elsewhere [36].

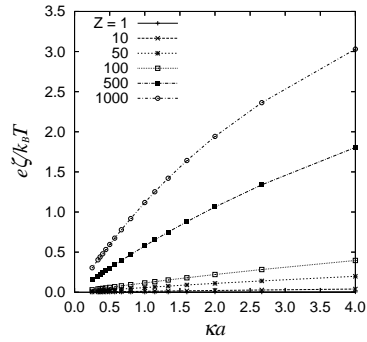


Fig. 5. Non-dimensionalized zeta potential as a function of the inverse Debye length κa and the valence of the colloid Z which was computed with a semi-analytic formula of Ohshima–Healy–White [37]. Lines are eye-guide only.

5 Conclusions

We presented a new simulation scheme for colloidal dispersions in a solvent of a multi-component fluid, which we call “Smoothed Profile (SP) method”. The SP method

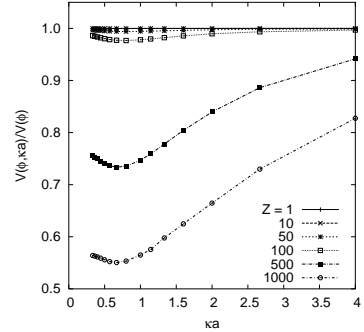


Fig. 6. Sedimentation velocity of a periodic array of colloids of different valences Z in an electrolyte solutions as a function of inverse Debye length κa . The ordinate is reduced by the sedimentation velocity of neutral colloids of the same volume fraction of 0.008. The effective volume fraction including electric double-layer defined by $(4/3)\pi\{(a + \kappa^{-1})/L\}^3$ was chosen to be less than unity. Lines are eye-guide only.

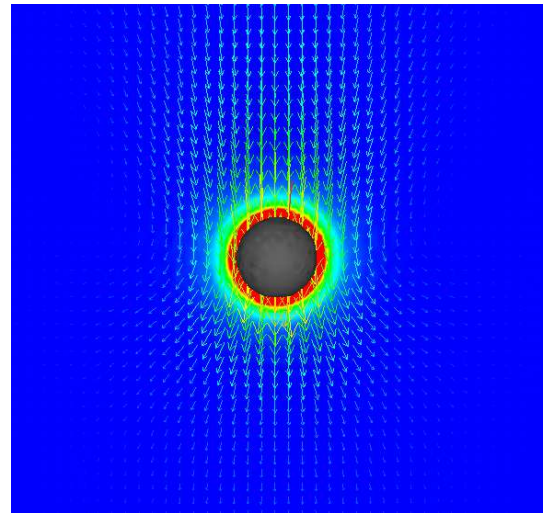


Fig. 7. Snapshot of the sedimenting charged colloid when $\kappa a = 1$ and $Z = 1000$. The arrows indicate the velocity field. The color around the particle represents the charge density field: change of color from red to blue corresponds to high to low charge density.

accomplishes improvement and extension from the previously proposed one by the authors [38,20,39].

The description of the colloidal systems is based on the Navier–Stokes equation for the momentum evolution of the solvent flow, the advection-diffusion equation for the solute distribution, the rigid body description of colloidal particles, and dynamical coupling of all these elements. Based on the momentum conservation between the continuum solvent fluid and discrete rigid colloids, the time-integrated hydrodynamic force and torque are derived. This expression of the mechanical coupling between a fluid and particles is well-suited for numerical simulation where differential equations are discretized in time. With this formulation on solid-fluid interaction, standard discretization schemes for uniform fluids are utilized as it is; no care for solid-fluid boundary mesh is needed. Since the hydrodynamic interaction is solved through the direct simulation of the solvent fluid, many-body effect is fully resolved.

The ability of the SP method was assessed in various test problems including the cases not only of simple fluids, but also of charged colloids in electrolyte solutions. The results showed the SP method worked well to study dynamical behaviors of colloids. Although we have focused on the systems of spherical colloids in simple fluids and Poisson–Nernst–Planck electrolytes (i.e. Poisson–Boltzmann level description of electrolytes), application to other types of macromolecules of any shapes, like disks [19], rods, and more, and other constitutive models for solvents is straightforward.

References

1. J. Happel, H. Brenner, *Low Reynolds number hydrodynamics: with special applications to particulate media*, 2nd edn. (Martinus Nijhoff, Dordrecht, 1983)
2. S. Kim, S.J. Karrila, *Microhydrodynamics : principles and selected applications* (Butterworth-Heinemann, London, 1991)
3. W.B. Russel, D.A. Saville, W.R. Schowalter, *Colloidal Dispersions* (Cambridge University Press, Cambridge, England, 1989)
4. C.N. Likos, *Phys. Rep.* **348**, 267 (2001)
5. J.F. Brady, G. Bossis, *Annu. Rev. Fluid Mech.* **20**, 111 (1988)
6. A. Malevanets, R. Kapral, *J. Chem. Phys.* **110**, 8605 (1999)
7. H. Tanaka, T. Araki, *Phys. Rev. Lett.* **85**, 1338 (2000)
8. T. Kajishima, S. Takiguchi, H. Hamasaki, Y. Miyake, *JSME Int. J., Ser. B* **44**(4), 526 (2001)
9. H.H. Hu, N.A. Patankar, M.Y. Zhu, *J. Comput. Phys.* **192**, 427 (2001)
10. R. Glowinski, T.W. Pan, T.I. Hesla, D.D. Joseph, J. Périoux, *J. Comput. Phys.* **192**, 363 (2001)
11. A.J.C. Ladd, R. Verberg, *J. Stat. Phys.* **104**, 1191 (2001)
12. J.T. Padding, A.A. Louis, *Phys. Rev. Lett.* **93**, 220601 (2004)
13. M.E. Cates, K. Stratford, R. Adhikari, P. Stansell, J.C. De-splat, I. Pagonabarraga, A.J. Wagner, *J. Phys.: Condens. Matter* **16**, S3903 (2004)
14. V. Lobaskin, B. Dünweg, C. Holm, *J. Phys.: Condens. Matter* **16**, S4063 (2004)
15. F. Capuani, I. Pagonabarraga, D. Frenkel, *J. Chem. Phys.* **121**, 973 (2004)

12 Yasuya Nakayama et al.: Simulating (electro)hydrodynamic effects in colloidal dispersions: smoothed profile method

16. Y.W. Kim, R.R. Netz, *Europhys. Lett.* **72**, 837 (2005)

17. A. Chatterji, J. Horbach, *J. Chem. Phys.* **122**, 184903 (2005)

18. T. Yamaue, M. Sasaki, T. Taniguchi, *Multi-Phase Dynamics Program “Muffin” User’s Manual*, <http://octa.jp> (2005)

19. F. Capuani, I. Pagonabarraga, D. Frenkel, *J. Chem. Phys.* **124**, 124903 (2006)

20. Y. Nakayama, R. Yamamoto, *Phys. Rev. E* **71**, 036707 (2005)

21. L.D. Landau, E.M. Lifshitz, *Fluid mechanics* (Pergamon Press, London, 1959)

22. C.S. Peskin, D.M. McQueen, *J. Comput. Phys.* **81**, 372 (1989)

23. J. Dzubiella, H. Löwen, C.N. Likos, *Phys. Rev. Lett.* **91**, 248301 (2003)

24. H. Kodama, K. Takeshita, T. Araki, H. Tanaka, *J. Phys.: Condens. Matter* **16**, L115 (2004)

25. A.A. Zick, G.M. Homsy, *J. Fluid Mech.* **115**, 13 (1982)

26. H. Hasimoto, *J. Fluid Mech.* **5**, 317 (1959)

27. D.J. Jeffrey, Y. Onishi, *J. Fluid Mech.* **139**, 261 (1984)

28. R.C. Ball, J.R. Melrose, *Physica A* **247**, 444 (1997)

29. J.R. Melrose, R.C. Ball, *J. Rheol.* **48**, 937 (2004)

30. C.W. Beenakker, *J. Chem. Phys.* **85**, 1581 (1986)

31. R.F. Probstein, *Physicochemical Hydrodynamics : An Introduction*, 2nd edn. (John Wiley & Sons, New York, 2003)

32. F. Booth, *J. Chem. Phys.* **22**, 1956 (1954)

33. H. Ohshima, T.W. Healy, L.R. White, R.W. O’Brien, *J. Chem. Soc., Faraday Trans. 2* **80**, 1299 (1984)

34. J.L. Anderson, *Annu. Rev. Fluid Mech.* **21**, 61 (1989)

35. D. Long, A. Ajdari, *Eur. Phys. J. E* **4**, 29 (2001)

36. K. Kim, Y. Nakayama, R. Yamamoto, *Phys. Rev. Lett.* **96**, 208302 (2006)

37. H. Ohshima, T.W. Healy, L.R. White, *J. Colloid Interface Sci.* **90**, 17 (1982)

38. R. Yamamoto, *Phys. Rev. Lett.* **87**, 075502 (2001)

39. K. Kim, R. Yamamoto, *Macromol. Theory Simul.* **14**, 278 (2005)